A self-consistent model of shock-heated plasma in non-equilibrium states for direct parameter constraints from X-ray observations S5.12

Yuken Ohshiro (Univ. Tokyo, ISAS/JAXA), Hiroya Yamaguchi (ISAS/JAXA, Univ. Tokyo)
Hiromasa Suzuki (ISAS/JAXA), Shunsuke Suzuki (Aoyama Gakuin Univ. ISAS/JAXA),
and Yoshizumi Okada (Aoyama Gakuin Univ. ISAS/JAXA)

Supernova Remnant III
June 9th–16th, 2024 @ Crete, Greece
Email: **ohshiro-yuken@g.ecc.u-tokyo.ac.jp**

Summary

We present a self-consistent model of thermal X-ray emission from shock-heated plasmas that accounts for non-equilibrium conditions of both temperature and ionization. Given a shock speed and initial electron-to-ion temperature ratio, the model calculates the temperature and ionization state of each element by simultaneously solving the relaxation processes. The thermal X-ray spectrum is synthesized by coupling our model with the AtomDB spectral code and compared with the *nei* model, a constant-temperature non-equilibrium ionization model commonly used in X-ray astronomy. The differences in emission line intensities between the models are significant enough to be distinguished even with a CCD detector. We find that the estimated ionization degree by *nei* model is systematically 30-40% lower than that predicted by our model. Implemented in the standard X-ray analysis software XSPEC, our model allows the physical parameters of shock-heated plasmas to be constrained directly from observations. Applying our model to the archival Chandra data of the supernova remnant N132D, we obtained a shock speed of 800 km s^{-1}, consistent with previous optical studies.

Introduction

- Non-equilibrium of ionization and temperature are often observed in Shock-heated plasmas in supernova remnants (SNRs) [e.g., 1, 2].
- Considering these non-equilibrium states is crucial for estimating parameters such as shock speed and ionization degree from X-ray observations (Fig. 1).
- However, conventional spectral models (e.g., *nei*, *pshock*) make the simplifying assumption of a constant electron temperature.

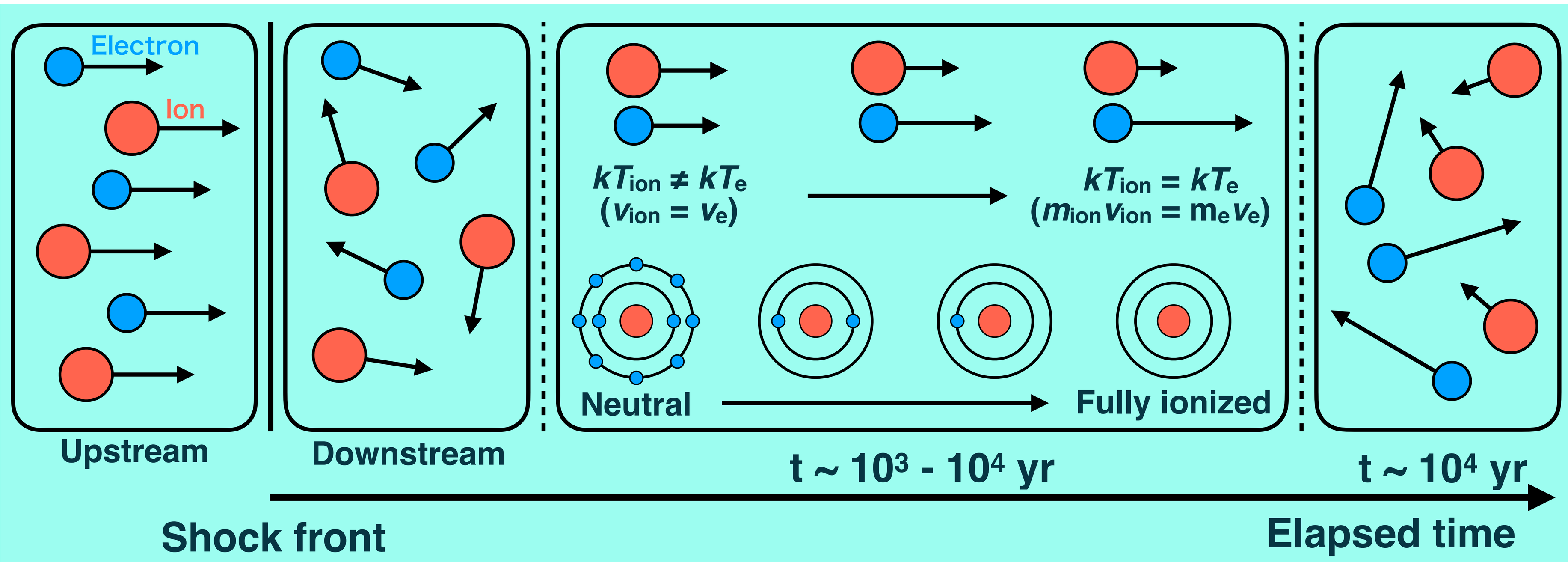

Fig. 1: Schematic view of shock heating and subsequent non-equilibrium processes.

Method

- For a given set of shock speed ($V_{\rm sh}$) and initial electron-ion temperature ratio ($\beta \equiv kT_{\rm e}/kT_{\rm ion}$), we numerically integrate ...

(1) Thermalization (see [2] for full expression)

$$\frac{{\rm d}(kT_i)}{{\rm d}(n_{\rm e}t)} = \sum_j \frac{kT_j - kT_i}{t_{{\rm eq},ij}}, \quad t_{{\rm eq},ij} \propto Z_i^{-2} Z_j^{-2} \left(\frac{kT_i}{m_i} + \frac{kT_j}{m_j} \right)^{3/2}$$

kT_i: temperature, m_i: mass, Z_i: mean charge number, $n_{\rm e}$: electron number density

(2) Ionization (generally used form, e.g., [3])

$$\frac{{\rm d}f_{X,x}}{{\rm d}(n_{\rm e}t)} = S_{X,x-1}(T_{\rm e})f_{X,x-1} - \{S_{X,x}(T_{\rm e}) + \alpha_{X,x}(T_{\rm e})\}f_{X,x} + S_{X,x+1}(T_{\rm e})f_{X,x+1}$$

$f_{X,x}$: ion fraction, $S_{X,x}$ ($\alpha_{X,x}$): ionization (or recombination) coefficients

- We adopt $\tau \equiv \int_0^t n_{\rm e}\,{\rm d}t$ as the integration variable.

Results

Calculation of solar abundance plasma

- Initial conditions & assumptions
  - $V_{\rm sh} = 1000$ km/s, $\beta = 0.01$
    $kT_i(\tau = 0) \sim \frac{3}{16} m_i V_{\rm sh}^2 \sim$ few keV
  - Singly ionized for all atoms
    $f_{X,1}(\tau = 0) = 1.0$
    $f_{X,x}(\tau = 0) = 0 \ (x \neq 1)$
  - Atoms ranging from H to Ni are considered with solar abundance
- The *nei* model shows faster ionization than our model due to the assumption of the constant $kT_{\rm e}$.
- The Fe^{+16} fraction ratio of our model to the nei model are 1.6 at $\tau = 10^{11}$ cm^{-3} s → Therefore, there are systematic biases in estimation of τ using the *nei* model.

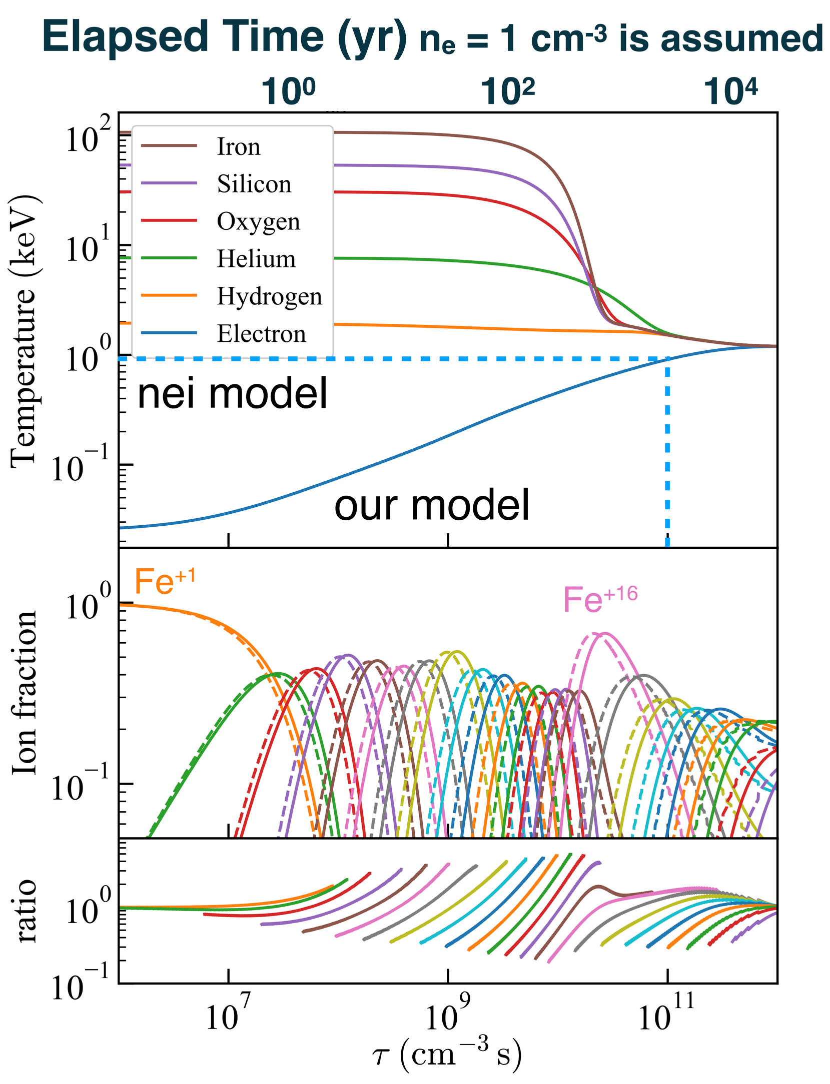

Fig. 2: The temporal evolution of temperatures and Fe ion fractions, and ion fractions ratios of our model and the *nei* model.

How did we compare our model with the *nei* model?

- To calculate ion fractions with the nei model, two parameters (i.e, $kT_{\rm e}$ and τ) are required. So we used the $kT_{\rm e}$ at each τ value obtained from our calculation (e.g., $kT_{\rm e} = 0.91$ keV at $\tau = 10^{11}$ cm^{-3} s).

Synthesized X-ray spectra

- Using AtomDB spectral code, which is widely used in X-ray astronomy.
- The emission line intensities of each models are different (Fig. 3), reflecting differences in ion fractions as shown in Fig. 2

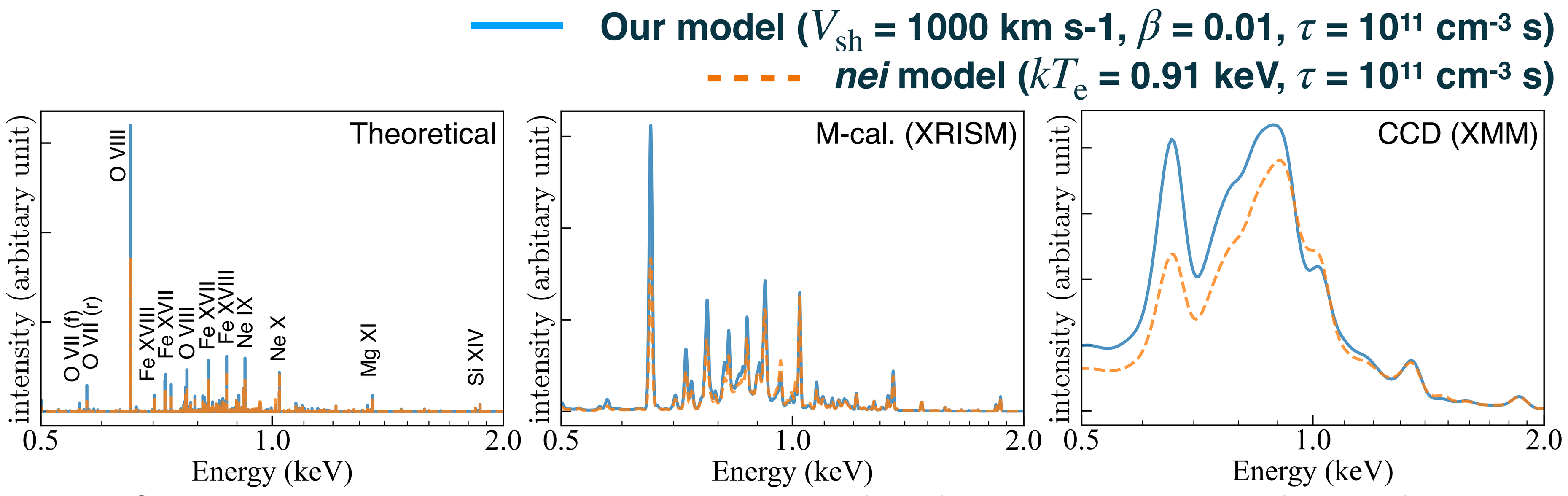

Fig. 3: Synthesized X-ray spectra using our model (blue) and the *nei* model (orange). The left shows the theoretical spectra, while the middle and right show the spectra convolved with instrumental responses of XRISM and XMM-Newton, respectively.

Systematic bias in parameter estimation using the *nei* model

- We calculate the O VIII Lyα emissivity as a function of τ using the *nei* model (Fig. 4), and search for the τ value at which both emissivities coincide by reducing the τ value of the *nei* model.
- The O VIII Lyα emissivity of our model can be explained by the *nei* model with $kT_{\rm e}$ = 0.91 keV, $\tau = 7.2 \times 10^{10}$ cm^{-3} s (Fig. 5).
- However, other emissivities (e.g., Fe XVII 3C and Ne IX resonance) does not match.
- Similar discrepancies are found to occur with corrections using other line emissivities (i.e., Fe XVII 3C and Ne IX resonance).
- This discrepancy suggests that systematic errors of < 20% also exist in abundance estimation using the *nei* model.

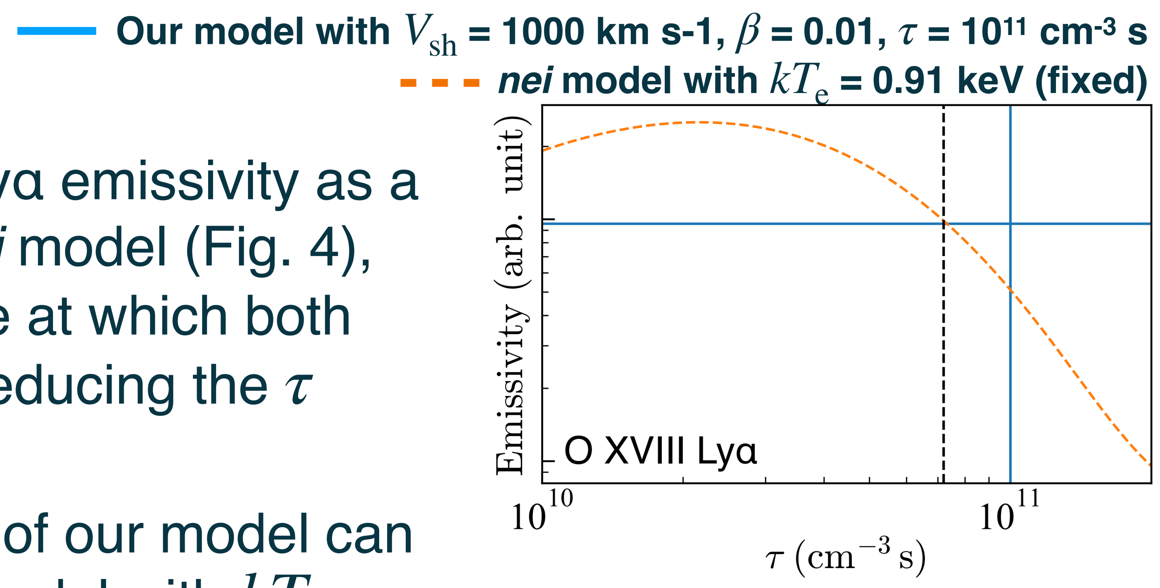

Fig. 4: Emissivity of O XVIII Lyα.

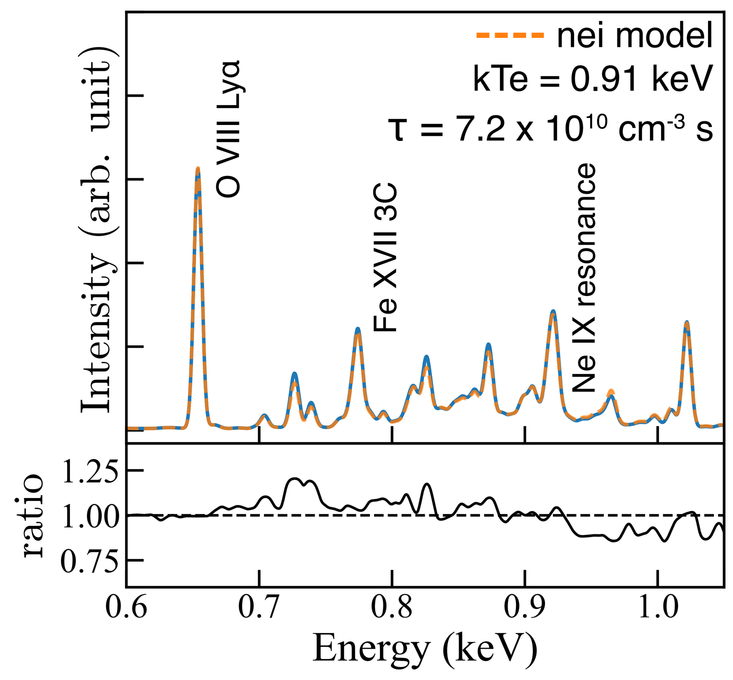

Fig. 5: (top) The modified *nei* spectrum. (bottom) Comparison with our model.

Applications to X-ray Observations

- Our model provides takes $V_{\rm sh}$, β and τ as inputs and outputs the synthesized spectrum.
- Therefore, our model can directly estimate these parameters from X-ray spectral fitting.
- As a demonstration, we applied our model to Chandra observations of N132D. We analyzed three outer rim regions (Fig. 6 and 7).
- The obtained shock speed of ~ 800 km/s is consistent with the previous optical study (Morse+1996).

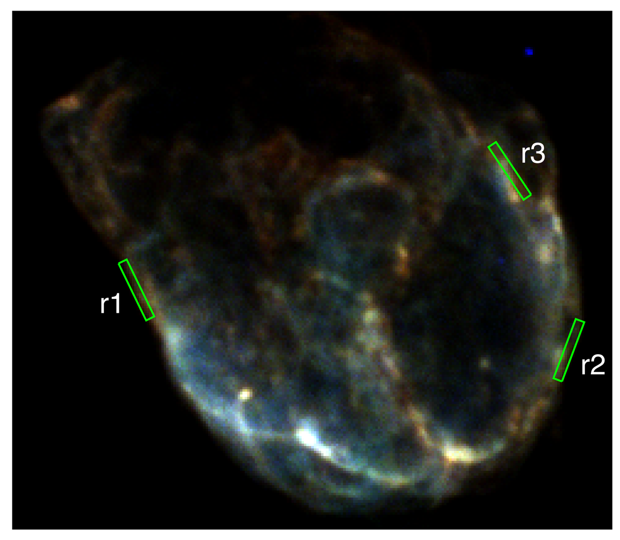

Fig. 6: An X-ray image of N132D.

our model	$V_{\rm sh}$ (km s^{-1})	τ (10^{11} cm^{-3} s)
r1	816^{+20}_{-16}	$2.34^{+0.28}_{-0.27}$
r2	884^{+22}_{-18}	$1.96^{+0.21}_{-0.20}$
r3	879^{+13}_{-11}	$2.62^{+0.21}_{-0.20}$
nei model	**$kT_{\rm e}$ (keV)**	**τ (10^{11} cm^{-3} s)**
r1	$0.75^{+0.03}_{-0.02}$	$2.10^{+0.34}_{-0.29}$
r2	$0.88^{+0.02}_{-0.03}$	$1.51^{+0.20}_{-0.16}$
r3	$0.88^{+0.02}_{-0.01}$	$2.09^{+0.19}_{-0.20}$

Tab. 1: Best-fit values. $\beta = m_{\rm e}/m_{\rm p}$ (fixed)

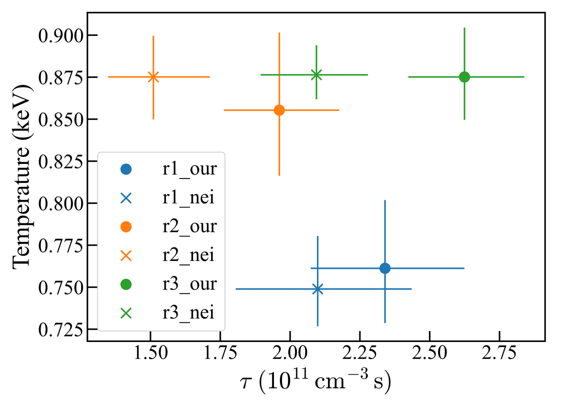

Fig. 8: Comparison between our model and the *nei* model.

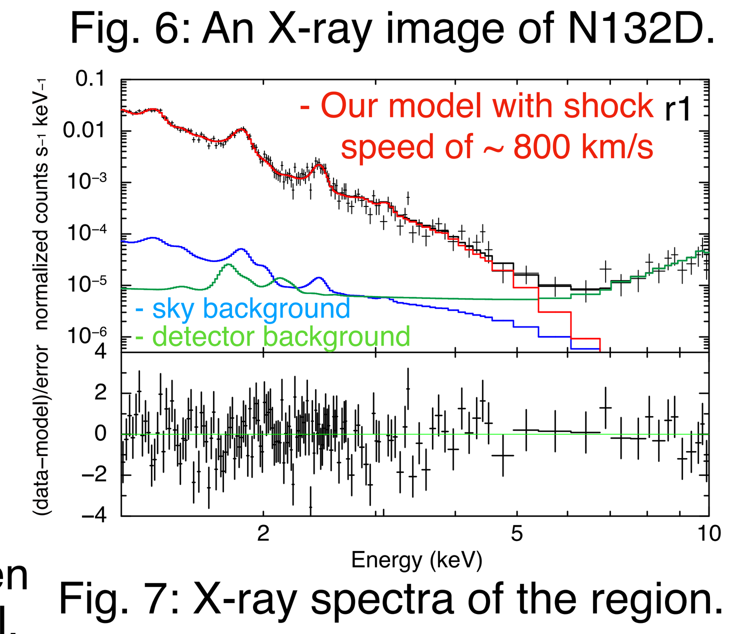

Fig. 7: X-ray spectra of the region.

References

[1] Yamaguchi, H., & Ohshiro, Y. 2022, in Handbook of X-ray and Gamma-ray Astrophysics, 1–17, [2] Vink, J. 2020, Physics and Evolution of Supernova Remnants, [3] Spitzer, L. 1956, Physics of Fully Ionized Gases, [4] Hamilton et al. 1983, ApJS, 51, 115, [5] Morse et al. 1996, ApJ, 112, 509